

Analysis for Enhancing the Performance Characteristics of Honeycomb-Filled Tubes at Constant Mass



Abdennour Benhizia^{*}, Abdelghani Khennab, Ilyas Bensalem

Mechanics of Structures and Materials Laboratory, University of Batna 2, Batna 05000, Algeria

Corresponding Author Email: a.benhizia@univ-batna2.dz

<https://doi.org/10.18280/rcma.330307>

ABSTRACT

Received: 9 January 2023

Accepted: 15 June 2023

Keywords:

compressive performance, energy absorption, filler material, honeycomb sandwich tubes, lightweight

In this paper, assuming the lightweight design is the main requirement, an efficient design of honeycomb sandwich tubes and its quasi-static compressive properties improvement were presented. The structures are designed in SolidWorks software, consisting of two face sheets and a honeycomb core implemented in its in-plane position. The axial compression tests are performed using Abaqus software. Detailed deformation features and energy absorption characteristics during the crushing process were presented. The compressive properties of the improved structures were determined from the energy absorption efficiency curves. Additionally, mathematical formulas for predicting the quasi-static compressive properties are presented. Theoretical predictions and FEA findings were in good agreement. In comparison to the standard structure, the suggested method greatly increased the structure's strength without adding mass to the design.

1. INTRODUCTION

Improving the compressive performance of thin-walled tubes by changing the section shapes has become saturated due to the limitations of material forming processes [1]. Therefore, many efforts have been made to develop new designs, such as composite tubes that combine thin-walled metal tubes with other parts, which show many favorable properties [1]. The investigated components include lattice [2-5], foam [6-9], honeycomb [10-13], fold [14], ortho-grid [15, 16], circumferential [17], and longitudinal corrugated [18, 19] cores. It was demonstrated that the dual-bearing capacity of tube and foam improve the overall stability and mechanical performance of the combined structure [20].

Honeycomb-filled structures have also been suggested as a filler to benefit from the interaction between thin-walled tubes and honeycombs. Wang et al. [21] analyzed the mechanical characteristics of honeycomb-filled thin-walled tubes, using experimental and computational methods. Mechanical properties and energy absorption properties were determined for various HFST samples with different geometric shapes. A correlation was observed between the honeycomb core and the thin-walled metal structure.

The study [22] investigated numerically the mechanical response of fluted-core sandwich cylinders under quasi-static uniaxial compression load. The findings showed that sandwich cylinders with a low cell number were more susceptible to local buckling, which decreases the compression performance. This could be effectively improved by increasing the number of cells and the wall thickness.

The study [23] analyzes numerically the properties of single and bitubular polygonal tubes packed with honeycomb for energy absorption. The findings demonstrate that single tubes packed with honeycomb have greater energy absorption

properties than tubes with various geometrical layouts. The study [24] examines the lateral planar crushing and bending responses of an aluminum honeycomb-filled square carbon fiber reinforced plastic (CFRP) tube. As a result of lateral crushing, the filled tubes were able to absorb 6.56 and 4 times more energy than hollow tubes without fillings.

In most of the mentioned literature the properties of the combined structure increase with the increasing density of the filling material. However, an increase in density increases the structure weight, which is an unfavorable point in the lightweight design. Additionally, the honeycomb core is implemented in its out-of-plane position [25]. From a mechanical point of view, the out-of-plane position loses the main characteristic of cellular materials under compression, which is the progressive cell collapse, which controls significantly the deformation mechanism. Moreover, in most numerical modeling of honeycomb sandwich tubes under compression, the densification step is not addressed [22] due to difficulties encountered, such as instabilities and excessive distortion at large deformations. This remains the principal obstacle limiting the exploration of complex design material.

As observed in the above literature, achieving the improvement of the energy absorption performance of honeycomb-filled tubes is still challenging. Therefore, this work was aimed at studying the improvement of compressive performance under quasi-static compression of honeycomb sandwich tubes with two factors: at a constant mass and up to the densification range of deformation frequently employed in engineering applications of cellular materials.

The compressive properties and energy-absorbing capability of designed honeycomb sandwich tubes are investigated and compared. Finally, the improved typical compressive properties are expressed. The paper is structured as follows:

- The honeycomb sandwich tube structure modeling is presented in section 2.
- The numerical results of the quasi-static compression tests are given and analyzed in section 3.
- The conclusions are reported in section 4.

2. MATERIALS AND METHODS

2.1 Geometry

As shown in Figure 1, the 3D model of a honeycomb sandwich structure consisting of two face sheets and a honeycomb core implemented in its in-plane position is designed in SolidWorks software.

The face sheet has a thickness of 1mm and a size of $110.07 \times 127.1 \text{ mm}^2$, and the honeycomb core has 2mm of cell wall thickness and 10mm of cell lateral length.

To create a cylindrical honeycomb sandwich part, the Flex tool available in Solidworks is used to bend the designed honeycomb sandwich structure and then duplicated to get the closed model, as shown in Figure 2. The advantage of the proposed method is the directly obtained of a 3D model of honeycomb-filled double circular tubes.

As discussed in the introduction, the compression performance of the studied honeycomb sandwich tubes is improved at a constant density. To this end, the honeycomb cell size was manipulated to create new structures containing more cells, keeping the same dimension and density as in the original structure (named L), as shown in Figure 3.

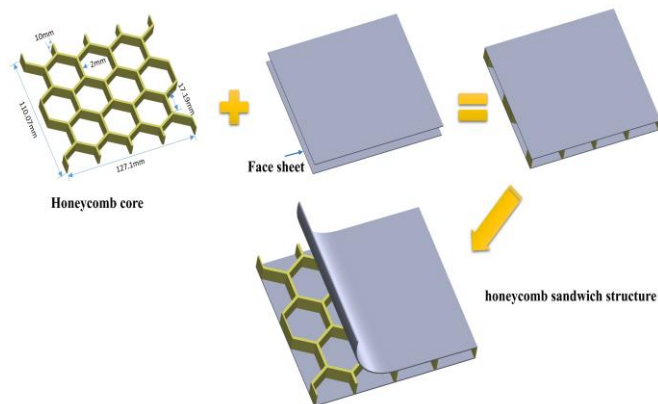


Figure 1. Designed honeycomb sandwich panel structure

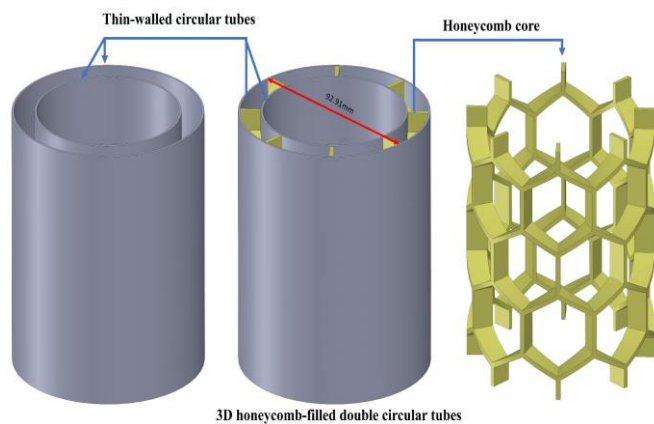


Figure 2. Schematic illustration of the created cylindrical honeycomb sandwich structure

Two modifications are adopted in this study:

- Adding half of the overall honeycomb structure to the original one, as illustrated in Figure 3(a) (naming it 1.5L), and then scaling it with a scale factor of 0.667 to get the original dimensions ($110.07 \times 127.1 \text{ mm}^2$), as illustrated in Figure 3(b).
- Adding the total of the overall honeycomb structure to the original one in the two directions, as illustrated in Figure 3(a) (naming it 2L), and then scaling it with a scale factor of 0.5 to get the original dimensions ($110.07 \times 127.1 \text{ mm}^2$), as illustrated in Figure 3(b).

The measured relative density in the three structures: L, 1.5L, and 2L, respectively is 0.12, which eliminates the relative density effect.

Figure 4 and Figure 5 represent the designed honeycomb sandwich structures and the created cylindrical honeycomb sandwich.

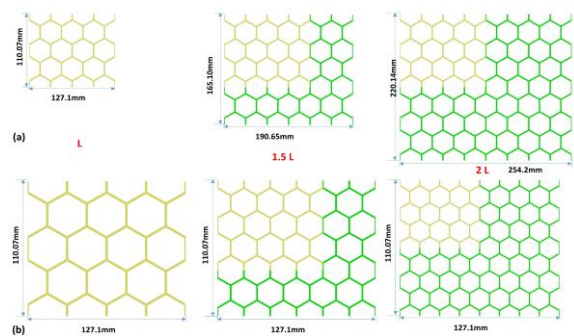


Figure 3. New structures containing more cells, and the same dimension and density as in the original structure (a): before the scale and (b) after the scale

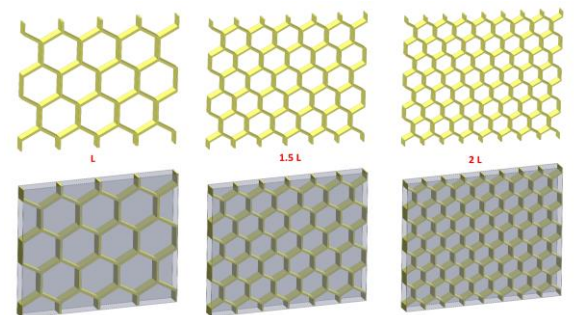


Figure 4. Schematic illustration of honeycomb sandwich structures designed with an increased number of cells and constant dimensions

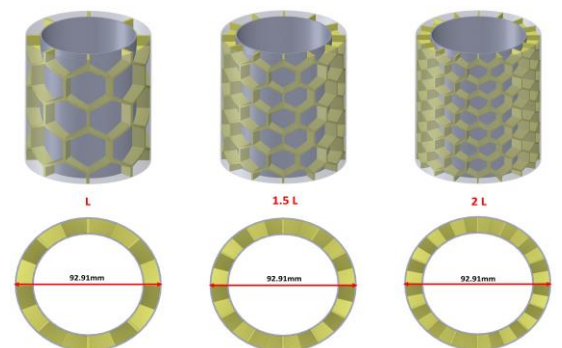


Figure 5. Cylindrical honeycomb sandwich structures designed with an increased number of cells and constant dimensions

2.2 Quasi-static axial compression loading

To evaluate the mechanical performance of the designed models, the in-plane quasi-static compression tests are performed up to the densification step using ABAQUS/Explicit code. As shown in Figure 6, the constructed model was loaded at a constant speed of 13.2m/s [26] by a rigid moving top plate while being maintained by a restrained rigid plate.

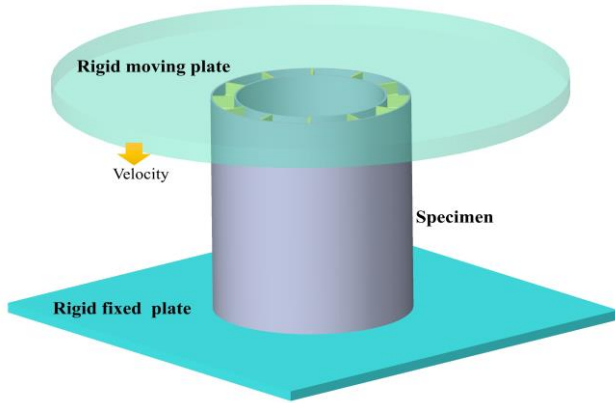


Figure 6. Illustration of the compression test configuration

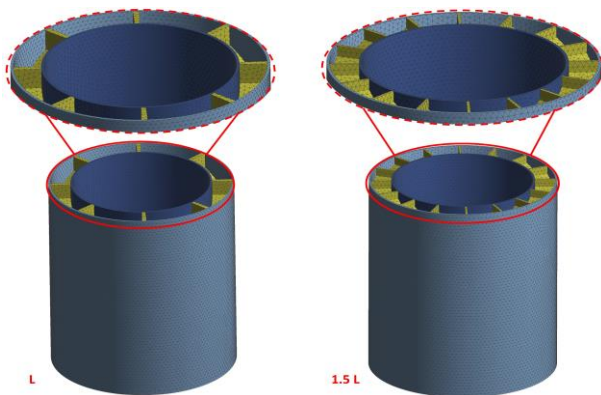


Figure 7. Illustration of 3D FE models

Table 1. Material properties used in finite element simulation [27]

Density (kg/m ³)	2710
Young's Modulus (GPa)	69
Yield Stress (MPa)	49.75
Poisson's Ratio	0.3
Stress (MPa)	Plastic strain
49.75	0
54.4	0.00539
63.69	0.0135
70.47	0.0216
76.53	0.0327
84	0.0529
90.39	0.0761
96.05	0.102
104.87	0.156
107.33	0.174
110.81	0.22
112.84	0.268
111.31	0.3
109.84	0.326

The geometric models have been discretized using tetrahedral elements with a size mesh of 1mm, as shown in Figure 7.

The Aluminum material was used for all components with the mechanical properties given in Table 1.

3. RESULTS AND DISCUSSIONS

3.1 Deformation patterns

The responses of the tested 3D models under compression test are shown below (Figures 8, 9, 10, 11, 12, and 13) with an illustration of the crushing pattern and Von Mises stress distribution. The advantage of numerical modeling is that it can illustrate the detailed deformation process of inner parts, such as the honeycomb core and inner facesheet, which could not be captured during an experimental test.

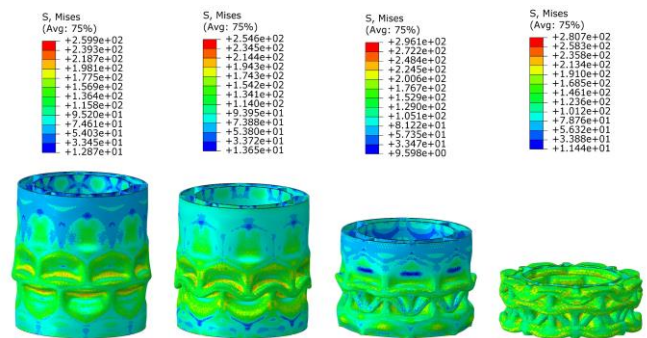


Figure 8. Deformation pattern and von mises stress distribution in the original structure L during the compression test

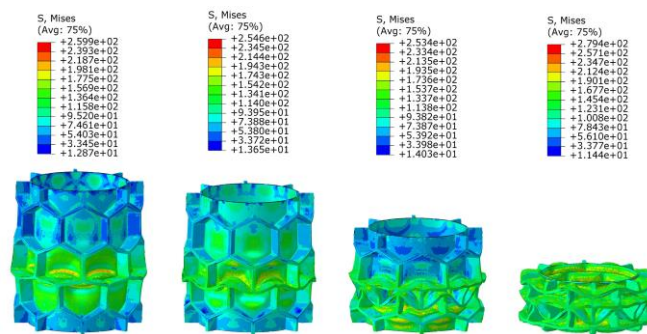


Figure 9. Captured deformation pattern in the internal geometry of the original structure L

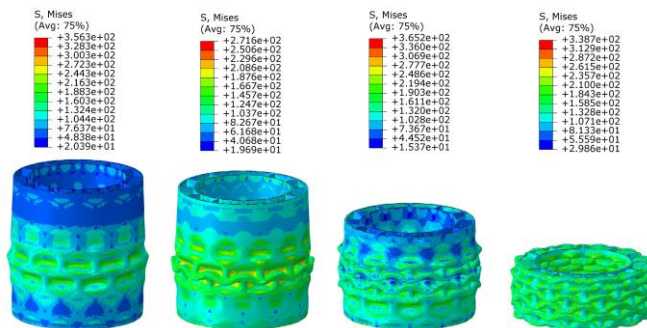


Figure 10. Deformation pattern and von mises stress distribution in the half-duplicated structure 1.5 L during the compression test

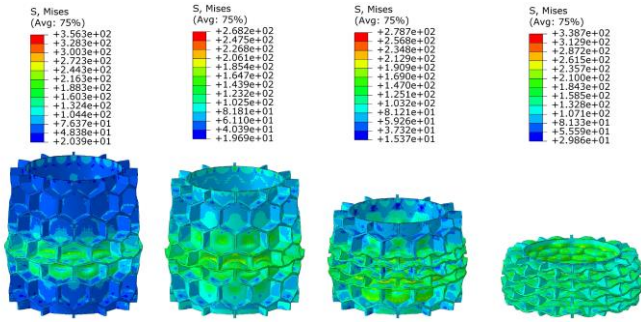


Figure 11. Captured deformation pattern in the internal geometry of the half-duplicated structure 1.5L

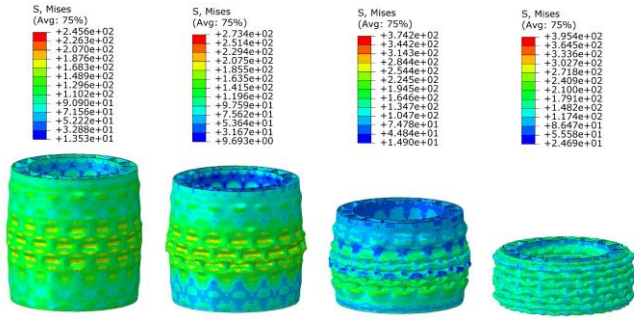


Figure 12. Deformation pattern and von misses stress distribution in the total-duplicated structure 2L during the compression test

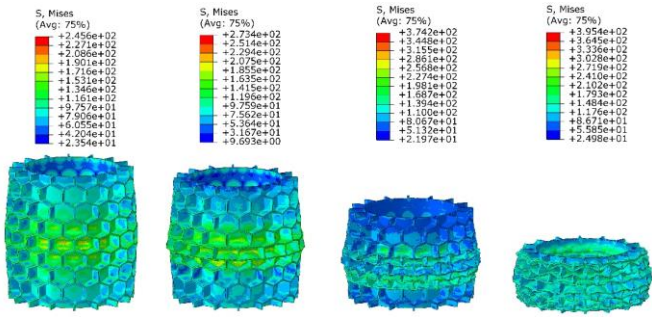


Figure 13. Captured deformation pattern in the internal geometry of the total-duplicated structure 2L

Figures 8, 9, 10, 11, 12, and 13 show how the folds formed are directly related to the honeycomb cells when the honeycomb is added to the tube as a filler. The fold has appeared in the weak zone of the cell, which is the upper vertex of the hexagon. Consequently, the number of folds is influenced by the number of honeycomb cells, which is why the 2L structure has more folds compared to other structures.

As is clearly seen in these figures the collapse of the tubular structure is constrained by the deformation of the honeycomb cells.

The overall stability of the combined model under axial crushing is achieved by the continuous buckling mode of the cells of the honeycomb, this primarily makes the coupled structure achieve exceptional efficiency as energy absorbers.

3.2 Quasi-static characteristics

The resulting compression stress-strain curves for the three tested honeycomb-filled double circular tubes are displayed in Figure 14.

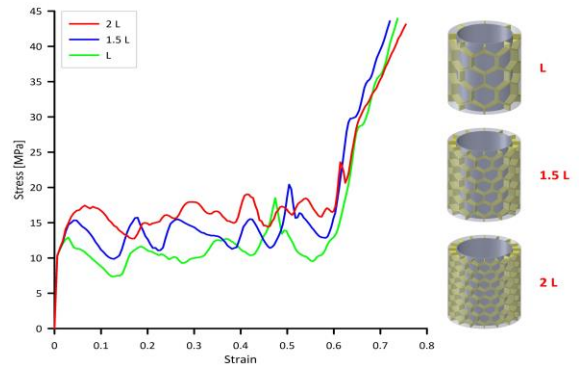


Figure 14. Resulting stress-strain compressive curves for the three tested honeycomb-filled double circular tubes

The stress-strain curves of the examined sandwich cylinders under uniaxial compression load display the common stages of cellular materials e.g., namely, short elastic stage, followed by a prolonged plateau stage, and finished by a densification stage.

The comparison shows a remarkable difference between the levels of the curves. The level increases when increasing the number of cells. The increased level implies an improvement in compression performance.

3.3 Determination of compressive properties

To best explore the obtained results, the compressive mechanical properties are extracted from the obtained stress-strain curves. The energy absorption efficiency was used to calculate the densification strain and plateau stress [28] of the tested models as follows:

$$\eta(\epsilon_a) = \frac{\int_0^{\epsilon_a} \sigma(\epsilon) d\epsilon}{\sigma_a}, 0 \leq \epsilon_a \leq 1 \quad (1)$$

The densification strain represents the highest peak in the energy absorption efficiency-strain curve given as:

$$\left. \frac{d\eta(\epsilon_a)}{d\epsilon} \right|_{\epsilon_a=\epsilon_d} = 0, 0 \leq \epsilon_d \leq 1 \quad (2)$$

The plateau stress σ_{pl} is calculated as:

$$\sigma_{pl} = \frac{\int_0^{\epsilon_d} \sigma(\epsilon) d\epsilon}{\epsilon_d} \quad (3)$$

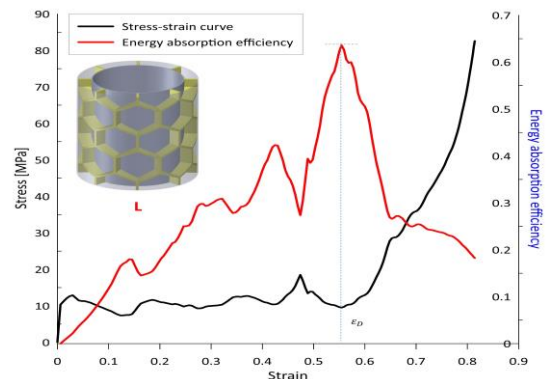


Figure 15. Efficiency-strain and stress-strain curves of original structure L

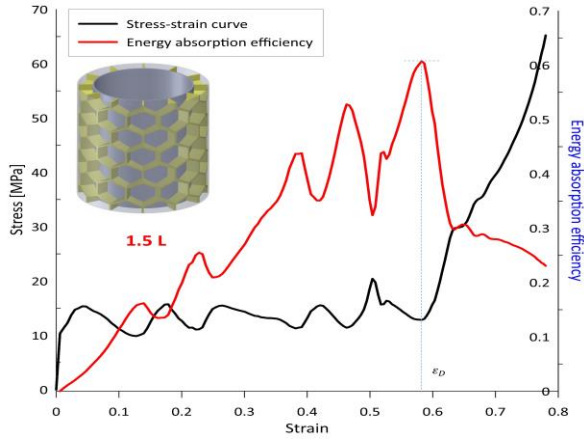


Figure 16. Efficiency-strain and stress-strain curves of half-duplicated structure 1.5 L

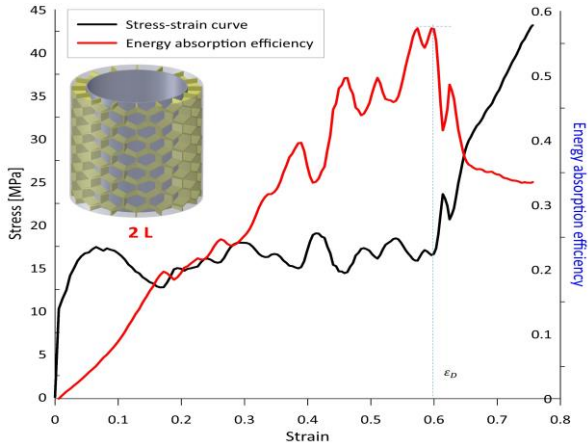


Figure 17. Efficiency-strain and stress-strain curves of total-duplicated structure 2L

Table 2 compares the calculated values of quasi-static characteristics.

Table 2. Calculated quasi-static characteristics for different configurations

Model	Collapse Stress (MPa)	Plateau Stress (MPa)	Densification Strain (%)
L	13.05	10.45	0.56
1.5 L	15.41	12.65	0.58
2 L	17.48	14.28	0.6

Figures 15, 16, and 17 display the efficiency-strain and stress-strain curves for the three designed models.

To analytically express the observed compressive mechanical properties, the correlation between these properties and the repeated dimension n could be described as:

Power law function for initial crush stress and plateau stress as:

$$\sigma = A(n)^B \quad (4)$$

Simple first-degree polynomial equation for densification strain as:

$$\varepsilon_D = \alpha + \beta(n) \quad (5)$$

The fitting parameters values of A , B , α , and β used are given in Table 3.

Table 3. Fitted parameter values

Collapse Stress (MPa)		Plateau Stress (MPa)		Densification Strain (%)	
A	B	A	B	α	β
13.036	0.421	10.49	0.448	0.5145	0.043

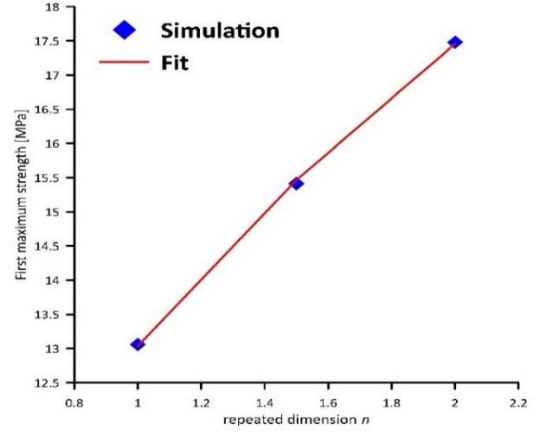


Figure 18. Comparison between collapse stress of fitted and numerical results

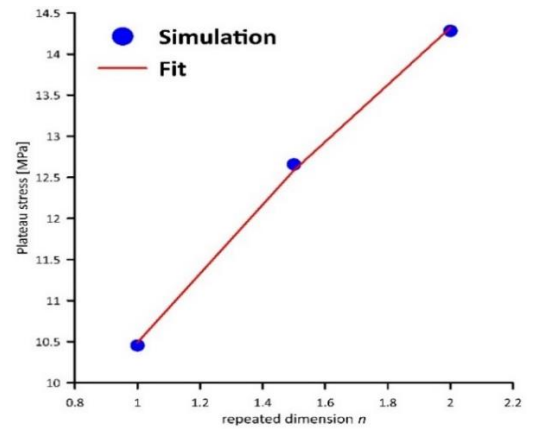


Figure 19. Comparison between plateau stress of fitted and numerical results

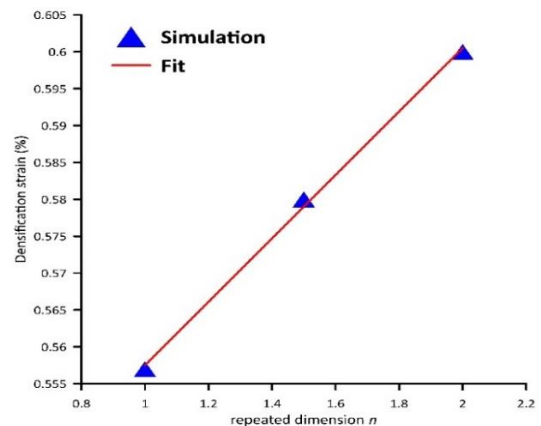


Figure 20. Comparison between densification strain of fitted and numerical results

Figures 18, 19, and 20 show the numerical findings along with the computed values using the suggested functions (Eq. (4) and Eq. (5)), respectively.

The numerical simulation results show that:

- The combined geometry interactions between the tubes and the honeycomb core led to an increase in crash resistance.
- The compressive strength increases with the increase of repeated dimension n .
- The predicted values using the proposed expressions showed good agreement with the FEA results.

4. CONCLUSIONS

In this study, honeycomb topology is suggested as a filler material to increase the compressive performance of tubular structures at constant density. 3D models of a cylindrical honeycomb sandwich structure are designed and investigated under quasi-static axial compression tests. Using Abaqus software, the axial compression tests are carried out. The obtained stress-strain compressive curves are used to determine the quasi-static compressive mechanical characteristics. The main conclusions were as follows:

- The honeycomb core structure changes the deformation mode of thin cylindrical tubes, giving them more stability and efficiency for energy absorption.
- Comparing the proposed strengthening approach to previous existing methods, it successfully enhanced the compressive performance without adding mass to the structure.
- The proposed analytical expressions linked the quasi-static compressive properties to the structural dimension, which can use to adjust the design for a given application.
- Based on the numerical results, the honeycomb structure was demonstrated as the best impact-resistant lightweight structure.

REFERENCES

- [1] Wu, F., Xiao, X., Dong, Y., Yang, J., Yu, Y. (2018). Quasi-static axial crush response and energy absorption of layered composite structure formed from novel crochet-sintered mesh tube and thin-walled tube. *Composite Structures*, 192: 592-604. <https://doi.org/10.1016/j.compstruct.2018.03.054>
- [2] Huang, W., Xu, H., Fan, Z., Jiang, W., Liu, J. (2020). Dynamic failure of ceramic particle reinforced foam-filled composite lattice core. *Composites Science and Technology*, 193: 108143. <https://doi.org/10.1016/j.compscitech.2020.108143>
- [3] Li, D., Qin, R., Xu, J., Zhou, J., Chen, B. (2022). Topology optimization of thin-walled tubes filled with lattice structures. *International Journal of Mechanical Sciences*, 227: 107457. <https://doi.org/10.1016/j.ijmecsci.2022.107457>
- [4] Cetin, E., Baykasoğlu, C. (2020). Crashworthiness of graded lattice structure filled thin-walled tubes under multiple impact loadings. *Thin-Walled Structures*, 154: 106849. <https://doi.org/10.1016/j.tws.2020.106849>
- [5] Baykasoğlu, A., Baykasoğlu, C., Cetin, E. (2020). Multi-objective crashworthiness optimization of lattice structure filled thin-walled tubes. *Thin-Walled Structures*, 149: 106630. <https://doi.org/10.1016/j.tws.2020.106630>
- [6] Salehi, M., Mirbagheri, S.M.H., Ramiani, A.J. (2021). Efficient energy absorption of functionally-graded metallic foam-filled tubes under impact loading. *Transactions of Nonferrous Metals Society of China*, 31(1): 92-110. [https://doi.org/10.1016/S1003-6326\(20\)65480-2](https://doi.org/10.1016/S1003-6326(20)65480-2)
- [7] Wang, L., Zhang, B., Zhang, J., Jiang, Y., Wang, W., Wu, G. (2021). Deformation and energy absorption properties of cenosphere-aluminum syntactic foam-filled tubes under axial compression. *Thin-Walled Structures*, 160: 107364. <https://doi.org/10.1016/j.tws.2020.107364>
- [8] Xue, Y., Mu, J., Huang, Y., Zhou, L., Shi, Z. (2021). Compressive mechanical properties of ex-situ auxetic composite-filled tubes. *Journal of Materials Research and Technology*, 14: 1644-1654. <https://doi.org/10.1016/j.jmrt.2021.07.061>
- [9] Linul, E., Khezzzadeh, O. (2021). Axial crashworthiness performance of foam-based composite structures under extreme temperature conditions. *Composite Structures*, 271: 114156. <https://doi.org/10.1016/j.compstruct.2021.114156>
- [10] Ghelloudj, E. (2020). Modeling and analysis the impact of unsymmetrical bending on aluminum honeycomb sandwich beams with polyester resin/glass fibers using finite element method. *Revue des Composites et des Matériaux Avancés-Journal of Composite and Advanced Materials Avancés*, 30(3-4): 181-188. <https://doi.org/10.18280/rcma.303-409>
- [11] Gupta, K., Chakraborti, P., Bhowmik, C. (2020). Study of modal behavior of sandwich structure with various core materials an analytical approach. *Revue des Composites et des Matériaux Avancés-Journal of Composite and Advanced Materials*, 30(1): 15-21. <https://doi.org/10.18280/rcma.300103>
- [12] Djemai, H., Labed, A., Hecini, M., Djoudi, T. (2021). Delamination analysis of composite sandwich plate of cork agglomerate/glass fiber-polyester: An experimental investigation. *Journal of Composite & Advanced Materials/Revue des Composites et des Matériaux Avancés*, 31(4): 193-197. <https://doi.org/10.18280/rcma.310402>
- [13] Zhao, C., Li, Y., Lu, Q. (2022). Study on seismic performance of honeycomb stiffened rib shaped concrete filled steel tube columns. *Case Studies in Construction Materials*, 17: e01534. <https://doi.org/10.1016/j.cscm.2022.e01534>
- [14] Du, Y., Song, C., Xiong, J., Wu, L. (2019). Fabrication and mechanical behaviors of carbon fiber reinforced composite foldcore based on curved-crease origami. *Composites Science and Technology*, 174: 94-105. <https://doi.org/10.1016/j.compscitech.2019.02.019>
- [15] Jiang, S., Sun, F., Fan, H., Fang, D. (2017). Fabrication and testing of composite orthogrid sandwich cylinder. *Composites Science and Technology*, 142: 171-179. <https://doi.org/10.1016/j.compscitech.2017.02.009>
- [16] Wu, H., Lai, C., Sun, F., Li, M., Ji, B., Wei, W., Liu, D., Zhang, X., Fan, H. (2018). Carbon fiber reinforced hierarchical orthogrid stiffened cylinder: fabrication and testing. *Acta Astronautica*, 145: 268-274. <https://doi.org/10.1016/j.actaastro.2018.01.064>
- [17] Xiong, J., Feng, L., Ghosh, R., Wu, H., Wu, L., Ma, L., Vaziri, A. (2016). Fabrication and mechanical behavior of carbon fiber composite sandwich cylindrical shells with corrugated cores. *Composite Structures*, 156: 307-

319. <https://doi.org/10.1016/j.compstruct.2015.10.009>
- [18] Boorle, R.K., Mallick, P.K. (2016). Global bending response of composite sandwich plates with corrugated core. Part II: Effect of laminate construction. *Composite Structures*, 141: 389-402. <https://doi.org/10.1016/j.compstruct.2016.01.040>
- [19] Su, P.B., Han, B., Yang, M., Wei, Z.H., Zhao, Z.Y., Zhang, Q.C., Zhang, Q., Qin, K.K., Lu, T.J. (2018). Axial compressive collapse of ultralight corrugated sandwich cylindrical shells. *Materials & Design*, 160: 325-337. <https://doi.org/10.1016/j.matdes.2018.09.034>
- [20] Liu, Z., Huang, Z., Qin, Q. (2017). Experimental and theoretical investigations on lateral crushing of aluminum foam-filled circular tubes. *Composite Structures*, 175: 19-27. <https://doi.org/10.1016/j.compstruct.2017.05.004>
- [21] Wang, Z., Yao, S., Lu, Z., Hui, D., Feo, L. (2016). Matching effect of honeycomb-filled thin-walled square tube-experiment and simulation. *Composite Structures*, 157: 494-505. <https://doi.org/10.1016/j.compstruct.2016.03.045>
- [22] Yang, H., Zhang, H., Li, X., Yin, L., Guo, X., Fan, H., Lei, H. (2022). Load-bearing capacity and failure mechanism of integrated fluted-core composite sandwich cylinders. *Composites Science and Technology*, 221: 109344. <https://doi.org/10.1016/j.compscitech.2022.109344>
- [23] Yin, H., Wen, G., Hou, S., Chen, K. (2011). Crushing analysis and multiobjective crashworthiness optimization of honeycomb-filled single and bitubular polygonal tubes. *Materials & Design*, 32(8-9): 4449-4460. <https://doi.org/10.1016/j.matdes.2011.03.060>
- [24] Liu, Q., Xu, X., Ma, J., Wang, J., Shi, Y., Hui, D. (2017). Lateral crushing and bending responses of CFRP square tube filled with aluminum honeycomb. *Composites Part B: Engineering*, 118: 104-115. <https://doi.org/10.1016/j.compositesb.2017.03.021>
- [25] Del Rosso, S., Iannucci, L. (2020). On the compressive response of polymeric cellular materials. *Materials*, 13(2): 457. <https://doi.org/10.3390/ma13020457>
- [26] Sadjad, P., Mohammad-Hosseini, E., Sobhan, E.M. (2018). Crashworthiness of double-cell conical tubes with different cross sections subjected to dynamic axial and oblique loads. *Journal of Central South University*, 25(3): 632-645. <https://doi.org/10.1007/s11771-018-3766-z>
- [27] Taherkhani, B., Kadkhodapour, J., Anaraki, A.P., Saeed, M., Tu, H. (2020). Drop impact of closed-cell aluminum foam: Experiment and simulation. *Journal of Failure Analysis and Prevention*, 20: 464-469. <https://doi.org/10.1007/s11668-020-00843-8>
- [28] Zhao, Y., Ma, C., Xin, D., Sun, M. (2020). Dynamic mechanical properties of closed-cell aluminum foams with uniform and graded densities. *Journal of Materials Research*, 35(19): 2575-2586. <https://doi.org/10.1557/jmr.2020.157>

NOMENCLATURE

A	Fitting parameter
B	Fitting parameter
E	Young's Modulus, GPa
L	Dimensionless length
<i>n</i>	Repeated dimension
t	Thickness, mm

Greek symbols

σ	Stress, MPa
ε	Strain
η	Energy absorption efficiency
ρ	Density, kg/m ³
σ_c	Collapse stress, MPa
σ_{pl}	Plateau stress, MPa
ε_d	Densification strain, %
α	Fitting parameter
β	Fitting parameter